



TBX3 promotes melanoma migration by transcriptional activation of ID1 which prevents activation of E-cadherin by MITF

Journal:	<i>Journal of Investigative Dermatology</i>
Manuscript ID	JID-2020-0777.R2
Article Type:	Original Article
Date Submitted by the Author:	22-Jan-2021
Complete List of Authors:	<p>Peres, Jade; University of Cape Town, Human Biology Damerell, Victoria; University of Cape Town Faculty of Health Sciences, Department of Human Biology Chauhan, Jagat.; Ludwig Institute for Cancer Research, University of Oxford, Nuffield Department of Clinical Medicine Popovic, Ana; University of Cape Town Faculty of Health Sciences, Department of Human Biology Desprez, Pierre-Yves; California Pacific Medical Center, Research Institute Galibert, Marie-Dominique ; Univ Rennes, CNRS, IGDR (Institut de Génétique et Développement de Rennes) – UMR6290, Hospital University of Rennes (CHU Rennes), Department of Molecular Genetics and Genomics Goding, Colin; University of Oxford, Ludwig Institute Prince, Sharon; University of Cape Town, Human Biology</p>
Keywords:	Cancer Biology, Cell Migration, Gene Regulation, Transcription Factors, Melanoma

TBX3 promotes melanoma migration by transcriptional activation of ID1 which prevents activation of E-cadherin by MITF

Jade Peres¹, Victoria Damerell¹, Jagat Chauhan², Ana Popovic¹, Pierre-Yves Desprez³, Marie-Dominique Galibert⁴, Colin R. Goding² and Sharon Prince^{1,*}

Authors' Affiliations: ¹Department of Human Biology, Faculty of Health Sciences, University of Cape Town, Observatory, 7925, Cape Town, South Africa.

²Ludwig Institute for Cancer Research, University of Oxford, Nuffield Department of Clinical Medicine, Old Road Campus Research Building, Oxford OX3 7DQ, United Kingdom.

³California Pacific Medical Center, Research Institute, San Francisco, CA, United States of America.

⁴Univ Rennes, CNRS, IGDR (Institut de Génétique et Développement de Rennes) – UMR6290, Hospital University of Rennes (CHU Rennes), Department of Molecular Genetics and Genomics, F-35000 Rennes, France.

Keywords: TBX3, ID1, melanoma, MITF, E-cadherin.

***Corresponding author:** Sharon Prince, E-mail: sharon.prince@uct.ac.za, Fax: +27 21 448 7226.

ABSTRACT

In melanoma, a phenotype-switch from proliferation to invasion underpins metastasis, the major cause of melanoma-associated death. The transition from radial to vertical growth phase (invasive) melanoma is characterised by down-regulation of both E-cadherin (*CDH1*) and the microphthalmia-associated transcription factor (M-MITF, hereafter referred to as MITF) as well as the up-regulation of the key cancer-associated T-box transcription factor TBX3 and the PI3K signalling pathway. Yet whether and how these diverse events are linked remains poorly understood. Here we show that TBX3 directly promotes expression of ID1, a dominant-negative regulator of basic-helix-loop helix transcription factors, and that ID1 decreases MITFs binding and upregulation of *CDH1*. Significantly, we show that TBX3 activation of ID1 is necessary for TBX3 to enhance melanoma cell migration, and the mechanistic links between TBX3, ID1, MITF and invasion revealed here are reflected in their expression in human melanomas. Our results reveal that melanoma migration is promoted through a TBX3-ID1-MITF-E-cadherin axis, and that ID1-mediated repression of MITF activity may reinforce maintenance of an MITF^{Low} phenotype associated with disease progression and therapy resistance.

1
2
3
4
5
6
7
8
9
10
11
12
13
14
15
16
17
18
19
20
21
22
23
24
25
26
27
28
29
30
31
32
33
34
35
36
37
38
39
40
41
42
43
44
45
46
47
48
49
50
51
52
53
54
55
56
57
58
59
60

INTRODUCTION

Malignant melanoma is the most aggressive skin cancer because it tends to recur and metastasize rapidly to regional lymph nodes and to distant organs (Gil et al., 2019). The annual incidence of cutaneous melanoma has increased to around 3-6% and is considered the fastest growing cancer worldwide (Eggermont et al., 2014). Melanoma progresses through well-defined stages starting with the radial growth phase (RGP) where the tumour is confined to the epidermis followed by the vertical growth phase (VGP) when the cells invade the underlying dermis and progress rapidly to metastasise to other organs (Scolyer et al., 2020).

Metastatic melanoma has a poor prognosis with a 5-year survival rate of less than 50% (Lideikaitė et al., 2017). Treatment includes immune checkpoint blockers (anti-CTLA-4, anti-PD1 antibodies) and targeted therapies to the constitutively activated RAS-RAF-MEK-MAPK (vemurafenib, dabrafenib, trametinib) and PI3K-AKT3 pathways involved in driving melanoma progression and invasion (Kozar et al., 2019). While most patients initially respond to these inhibitors, a large proportion develop resistance and succumb to the disease (Domingues et al., 2018). For example, ~60% of patients develop resistance to anti-PD1 therapy (O'Donnell et al., 2017). A significant contribution to therapy resistance results from melanoma cells being highly plastic and capable of undergoing bi-directional switching between proliferative and invasive phenotypes (Rambow et al., 2019). MITF, a basic-helix-loop helix-leucine zipper (bHLH-LZ) transcription factor, co-ordinates many aspects of melanoma biology and is a key molecular marker used to distinguish between proliferative (MITF^{High}) and invasive (MITF^{Low}) melanoma phenotypic states (Goding and Arnheiter, 2019, Hoek et al., 2006).

TBX3 is an important developmental transcription factor that is frequently overexpressed in cancers, including a subset of melanomas, where it promotes proliferation, tumour formation in xenograft models, angiogenesis, metastasis and invasion (Khan et al., 2019). In melanoma, TBX3 levels and activity are upregulated transcriptionally and post-translationally by the BRAF^{V600E} and PI3K/AKT3 signalling pathways respectively that are both constitutively activated in approximately 60% of melanomas (Boyd et al., 2013, Dantonio et al., 2019, Peres et al., 2015). TBX3 contributes to melanoma formation and invasion by directly repressing *E-cadherin*, a cell-cell adhesion molecule that is characteristically downregulated during the transition to the invasive melanoma phenotype (Miller and Mihm, 2006, Rodriguez et al., 2008). The ability of TBX3 to repress E-cadherin is enhanced when it is phosphorylated by

AKT3, and is consistent with TBX3 being more highly expressed in VGP melanomas than in the RGP (Peres et al., 2010, Peres et al., 2015, Peres and Prince, 2013). Despite the importance of TBX3, its repertoire of target genes and its broader role in melanoma and other cancers remains largely unknown.

In the current study, we show that *ID1*, a dominant-negative bHLH factor and key regulator of cancer progression, is directly activated by TBX3 and that ID1 mediates TBX3-induced melanoma migration through a mechanism involving its ability to decrease MITF activity and thereby repress E-cadherin.

RESULTS

Identification of TBX3-regulated genes in VGP melanoma cells

To determine the molecular mechanism underpinning the role of TBX3 in melanoma, we established ME1402 shCtrl and shTBX3 cell lines using RNA interference and conducted a whole genome microarray with mRNA from four shCtrl and four shTBX3 clones (Figure 1a and 1b). A heat map and volcano plot (Figure 1c) show the differentially expressed relevant genes with a *p*-value cut-off of 0.05 and absolute mean log₂ ratio greater than one (fold change ≥ 2) (Supplementary Table S1). Importantly, TBX3 mRNA was confirmed to be downregulated in the shTBX3 cells and *CDH1* (*E-cadherin*), a target gene repressed by TBX3, was upregulated in these cells (Figure 1d).

When the 960 differentially expressed genes identified were grouped with their gene ontology (GO) terms, 259 genes associated with key hallmarks of cancer. Of particular interest were 13 genes (6 upregulated: *CDH1*, *LEPREL1*, *WNT3*, *HMCN1*, *NEDD4L*, *NCAM1* and 7 downregulated: *MMP1*, *MMP15*, *IGF1*, *NGFR1*, *FOXC2*, *EPHB3* and *ID1*) whose de-regulation was shown to promote tumour formation, migration and invasion (Supplementary Tables S2 and S3). The expression of these genes in the ME1402 shTBX3 cells was validated by qRT-PCR (Figure 1d). Furthermore, qRT-PCR experiments performed with RNA from WM1650 RGP cells engineered to overexpress TBX3 revealed that TBX3 overexpression regulated the 13 putative target genes in a reciprocal fashion to that observed using the shRNA (Figure 1e).

TBX3 is a direct transcriptional activator of *ID1*

1
2
3
4
5
6
7
8
9
10
11
12
13
14
15
16
17
18
19
20
21
22
23
24
25
26
27
28
29
30
31
32
33
34
35
36
37
38
39
40
41
42
43
44
45
46
47
48
49
50
51
52
53
54
55
56
57
58
59
60

Among the genes most significantly downregulated (7.2-fold; p-value 0,000292) when TBX3 was knocked down was *Inhibitor of differentiation 1 (ID1)* (Supplementary Table S3). ID1 associates with bHLH transcription factors rendering them transcriptionally inactive by preventing them from binding DNA (Roschger and Cabrele, 2017). Like TBX3, ID1 is overexpressed in melanoma as compared to human melanocytes and promotes melanoma invasion (Straume and Akslen, 2005, Zigler et al., 2011). However, the factors responsible for this upregulation and the repertoire of ID1 dimerization targets involved in this oncogenic function are not well characterized. We speculated that TBX3 may be responsible for transcriptionally upregulating *ID1*. Indeed, knockdown of TBX3 down-regulated ID1 in VGP cells (Figure 2a), while ectopic expression of TBX3 up-regulated ID1 in RGP cells (Figure 2b). Significantly, both *TBX3* (Figure 2c) and *ID1* (Figure 2d) mRNA expression strongly correlated with the Verfaillie invasive gene expression signature (Verfaillie et al., 2015) in the TCGA melanoma cohort ranked by the invasive signature.

While TBX3 repressed an *E-cadherin* promoter, it activated an *ID1* promoter (FL ID1) driving a luciferase reporter in a dose-dependent manner in two VGP cell lines (Figure 3a). This regulation was abolished when the TBX3 DNA binding domain was mutated (R133G TBX3 DBM) and when the activation domain (TBX3 N-terminal) was deleted (Figure 3b). Furthermore, we show that, despite being structurally different, the TBX3 and TBX3+2a isoforms are both capable of activating the *ID1* promoter suggesting that in this context they have functionally similar roles (Figure 3c). Western blotting confirmed similar expression levels of the TBX3 transfected proteins.

A T-element at -1986 bp in the *ID1* promoter mediates the activation by TBX3

To identify the region of the *ID1* promoter responsible for mediating activation by TBX3, a series of *ID1* promoter deletion mutants (Figure 3d) cloned upstream of a luciferase reporter were co-transfected with TBX3 in VGP cells. Figure 3d shows that compared to the FL *ID1* construct none of the deletion mutants were activated by TBX3. This suggests that the element(s) mediating activation of *ID1* promoter activity by TBX3 resides between -1572 bp and -2212 bp. Consistent with this, one highly conserved consensus T-element was identified at -1986 bp from the transcription start site and mutation of this element prevented activation of the *ID1* promoter by TBX3 (Figure 3e). The -1572 mutant was used as a control. These results confirmed that the consensus T-element at -1986 bp likely represents the site through which TBX3 binds and activates the *ID1* promoter. Indeed, this was confirmed in an

electrophoretic mobility shift DNA binding assay (EMSA) where nuclear extract from VGP cells were incubated with biotinylated oligonucleotides containing the WT T-element at -1986 bp (Figure 3f). Two bands representing protein binding were readily detected (lane 2) and neither of the two bands were competed efficiently by random non-biotinylated-labelled oligonucleotides (lane 3). Importantly, an antibody against TBX3 super-shifted the nuclear complexes on the oligonucleotides (lane 4). Furthermore, ChIP assays revealed that relative to the non-specific IgG control, there was a 3.31-fold enrichment of TBX3 occupancy on the *ID1* promoter but not at *GAPDH* (Figure 3g). Taken together, the data presented above suggest that TBX3 binds and directly activates *ID1*.

The AKT pathway enhances the ability of TBX3 to bind and activate the *ID1* promoter

Phosphorylation of TBX3 by AKT3 at S720 enhances its ability to repress *E-cadherin* (Peres et al., 2015). We therefore investigated the effect of TBX3 constructs in which S720 was either mutated to alanine (TBX3 S720A) to abolish phosphorylation or glutamic acid (TBX3 S720E) to mimic phosphorylation on FL *ID1* promoter activity. Whereas the WT-TBX3 and TBX3 S720E activated the *ID1* promoter, abolishing the AKT phosphorylation site (TBX3 S720A) abrogated this activation (Figure 4a). Similar protein expression was observed for the three TBX3 proteins tested. Furthermore, a DNA affinity immunoprecipitation (DAI) assay shows that TBX3 only bound to oligonucleotides carrying a WT *ID1* -1986 bp T-element, and that this binding was reduced when the cells were treated with the AKTVIII inhibitor (Figure 4b, upper panel). Western blotting confirmed the efficacy of the AKTVIII inhibitor (Figure 4b, lower panel). Furthermore, DAI assays revealed that whereas the WT-TBX3 and TBX3 S720E proteins bound the -1986 bp T-element, the TBX3 S720A protein showed reduced binding to this site (Figure 4c, upper panel). Western blotting show that similar protein expression was observed for each of the TBX3 constructs (Figure 4c, lower panel). Taken together these results suggest that phosphorylation of TBX3 by AKT3 at S720 also regulates its ability to activate and bind the *ID1* promoter.

TBX3 promotes cell migration through the activation of *ID1*

To test whether *ID1* may act downstream of TBX3 to promote migration, we first established whether *ID1* promotes migration of VGP cells which require TBX3 for migration (Peres et al., 2010). Results from scratch motility assays show that the depletion of *ID1* by two siRNAs (Figure 5a, upper panels) significantly inhibited the migration of these VGP cells by 24 hrs (Figure 5a, lower panels). Consistent with these data, *ID1* overexpression enhanced their

1
2
3
4
5
6
7
8
9
10
11
12
13
14
15
16
17
18
19
20
21
22
23
24
25
26
27
28
29
30
31
32
33
34
35
36
37
38
39
40
41
42
43
44
45
46
47
48
49
50
51
52
53
54
55
56
57
58
59
60

migration and, importantly, could rescue the decreased migration caused by depletion of TBX3 (Figure 5b). Furthermore, while WM1650-TBX3 cells migrated significantly faster than WM1650-Ctrl cells from 4 hrs, depleting ID1 in the WM1650-TBX3 cells significantly compromised their ability to migrate from 6 hrs (Figure 5c). These results show that ID1 is required for TBX3-induced melanoma cell migration.

ID1 prevents activation of *E-cadherin* by MITF

Since TBX3 can directly repress *E-cadherin* to promote melanoma cell migration and invasion (Peres et al., 2010, Peres et al., 2015, Peres and Prince, 2013, Rodriguez et al., 2008), we next investigated whether TBX3 can also downregulate *E-cadherin* through the activation of *ID1*. Figure 6a shows that TBX3 and ID1 play an important role in keeping E-cadherin levels low in two VGP cell lines; silencing either TBX3 or ID1 using two different siRNAs led to increased *E-cadherin* promoter activity. Importantly, when ID1 was overexpressed in si-TBX3 or shTBX3 VGP cells, the increase in *E-cadherin* promoter activity (Figure 6a), and endogenous mRNA and protein levels (Figure 6b) were abolished.

Previous studies in osteoclasts have suggested that ID1 can interact with the bHLH-LZ transcription factor, MITF (Lee et al., 2006), and that MITF can bind and activate *E-cadherin* through a conserved E-box motif at -103 bp (Mansky et al., 2002). We therefore hypothesised that ID1 inhibits E-cadherin expression in VGP cells by preventing MITF from activating *E-cadherin*. Indeed, immunoprecipitation assays confirmed that ID1 interacts with MITF (Figure 6c). Importantly, in the TCGA melanoma cohort (Figure 6d) and in a panel of 53 melanoma cell lines grouped according to their phenotype (Tsoi et al., 2018) (Figure 6e), MITF or a representative set of known MITF target genes tended to anti-correlate with ID1 expression. Moreover, examination of replicate MITF ChIP-sequencing data (Louphrasitthiphol et al., 2020) confirmed that MITF could bind the E-cadherin (*CDH1*) locus, but binding was observed in an intron at two consensus CATGTG elements (Figure 6f), and not within the *CDH1* promoter as previously described in osteoclasts. Importantly, ChIP assays reveal that when ID1 is depleted in VGP cells, there is a 5.46- and 5597.23-fold increase in MITF occupancy on these two intronic elements (Figure 6g). Together these results provide evidence that ID1 may promote VGP migration by preventing MITF from activating *E-cadherin*. To test this, we performed scratch motility assays on cells in which ID1 and MITF were overexpressed individually or together. As expected, overexpressing ID1 increased the migration of VGP cells. Importantly, overexpression of MITF alone inhibited their migration but when co-

expressed with ID1 this effect was abrogated (Figure 6h). Furthermore, the relationship between *MITF* and *E-cadherin* *in vivo* was explored by examining the RNA-sequencing gene expression data in the TCGA melanoma cohort. These data showed a clear positive correlation between *MITF* and *E-cadherin* expression (Figure 6i). Taken together, the data presented above suggest that ID1 promotes melanoma migration downstream of TBX3 through, in part, preventing MITF from activating E-cadherin.

DISCUSSION

Cutaneous malignant melanoma is the most lethal skin cancer and it is notoriously recalcitrant to standard anti-cancer regimes (Gil et al., 2019). In addition to genetic lesions, it is now increasingly recognised that a primary driver of invasion and drug tolerance is the impact of the intra-tumour microenvironment combined with melanoma cell plasticity (Kozar et al., 2019, Rambow et al., 2019). Understanding how mutations affecting intrinsic signalling pathways sensitize cells to extracellular cues to drive them to adopt a migratory and pro-metastatic phenotype is important, especially since melanoma therapy resistance and invasion are closely linked.

A key driver mutation of melanoma progression is loss of PTEN, that leads to greatly enhanced probability of cells in the primary tumour becoming invasive as a consequence of elevated PI3K signalling (Kozar et al., 2019). However, while the PI3K pathway has been linked to melanoma RGP to VGP transition and consequently to increased metastasis, as well as BRAF inhibitor (BRAFi) resistance, the downstream events that link PI3K signalling to invasion are poorly understood (Kozar et al., 2019).

In epithelial cancers, as in melanoma, the transition to invasion is associated with decreased E-cadherin expression (Miller and Mihm, 2006). This has been linked to transcription factors such as TWIST, ZEB and SNAIL which are associated with an epithelial-to mesenchymal transition (EMT) (Caramel et al., 2013, Poser and Bosserhoff, 2004). However, the focus on EMT-related events has meant that the key role of TBX3 has been frequently overlooked, despite the accumulating evidence that TBX3 is likely to play an equally important role. Indeed, TBX3 is sufficient to promote RGP melanoma cell migration, anchorage independent growth and tumour formation (Peres and Prince, 2013), and depleting TBX3 in invasive melanoma cells inhibits their migration and tumour forming ability (Peres et al., 2010). Yet how TBX3 might mediate these effects was not clear. Here we demonstrate that TBX3

1
2
3
4
5
6
7
8
9
10
11
12
13
14
15
16
17
18
19
20
21
22
23
24
25
26
27
28
29
30
31
32
33
34
35
36
37
38
39
40
41
42
43
44
45
46
47
48
49
50
51
52
53
54
55
56
57
58
59
60

transcriptionally activates *ID1*, an activity that is enhanced when it is phosphorylated by AKT3, a key driver of BRAFi resistance and melanoma invasion. Our observations indicate that ID1 is a TBX3 target downstream from PI3K signalling which may explain why it is more highly expressed in undifferentiated and invasive melanomas.

Importantly, we show that ID1 suppresses the activity of MITF, a critical coordinator of melanoma biology with MITF^{Low} cells tending to be invasive and therapy resistant (Goding and Arnheiter, 2019, Rambow et al., 2019). Here we link upstream PI3K signalling to down-regulation of MITF activity via TBX3 and its ability to activate ID1 expression. We also show that, consistent with MITF^{Low} cells being more invasive (Carreira et al., 2006), MITF binds *CDH1* and that there is a strong positive correlation between their expression in human melanomas.

Multiple stresses within the tumour microenvironment, including hypoxia, nutrient limitation and inflammation, are known to downregulate MITF transcriptionally and translationally (Cheli et al., 2012, Falletta et al., 2017, Feige et al., 2011, Landsberg et al., 2012, Louphrasitthiphol et al., 2019, Riesenberger et al., 2015). Our observation that ID1 can bind and possibly sequester MITF reveals an additional means by which MITF activity can be down-regulated. However, we cannot exclude the possibility that this may occur through ID1 acting on another protein partner that interferes with MITF binding at the E-boxes in *CDH1*. Since ID1 and MITF mRNA expression tend to be inversely correlated in both human melanomas and cell lines, the role of ID1 mediated inhibition of MITF activity may reflect a need of cells to down-regulate any residual MITF activity to enhance and maintain the clinically important MITF^{Low} phenotype.

In conclusion, we reveal that the AKT3-TBX3-ID1-MITF axis identified here plays an important role in promoting the migration of malignant melanoma cells. These findings may have important implications for the design of therapeutic strategies in malignant melanoma driven by this pathway.

MATERIALS AND METHODS

Cell culture and AKTVIII inhibitor treatments

The WM1650 (RGP), ME1402 (VGP) and MM200 (VGP) cells were derived from human melanomas and were sourced from the Wellcome Trust Functional Genomics Cell Bank

(Sviderskaya et al., 2010) and they were maintained as previously described (Peres et al., 2010). The molecular characteristics of these melanoma cell lines are shown in Supplementary Table S4. AKTVIII inhibitor treatments of cells were performed as previously described (Peres et al., 2015).

Microarray analysis

Gene expression profiling was performed using the Agilent SurePrint G3 Human GE 8x60K Microarray Kit (G4851A). Total RNA from ME1402 shCtrl and shTBX3 cell lines was reverse transcribed to cDNA using the One-Color RNA Spike-In Kit (5188-5282), followed by an *in vitro* transcription reaction to amplify and label complementary RNA (cRNA) with Cy3-CTP using the Low Input Quick Amp Labeling Kit (5190-2305). Cy3-labeled cRNA was hybridized to the microarray chips using the Gene Expression Hybridization Kit (5188-5242). Microarray slides were scanned on a dynamic autofocus Agilent G2565BA microarray scanner. The processed Multiplicative Detrend FE data (FE v9.4.1, GE1-v5_91_0806 protocol) was median normalised and missing values were imputed (Limma and impute, R packages). Significance in differential gene expression was determined using standard Student's t test of two groups. Adjusted P values were computed by controlling the false discovery rate (FDR) with the Benjamini & Hochberg (BH) procedure implemented in multi-test (R package). Differentially expressed genes were defined as follows: BH adjusted p value <0.05 and absolute mean log2 ratio greater than one (fold change ≥ 2).

Quantitative real-time PCR (qRT-PCR)

qRT-PCR was performed as previously described (Abrahams et al., 2008). Primers were *TBX3* (QT00022484; Qiagen), *E-cadherin* (QT00080143; Qiagen), *NCAM1* (QT00071211; Qiagen), and *GUSB* (QT00046046; Qiagen).

Plasmids

pCMV-TBX3 (WT-TBX3), pcDNA3-ID1, and pCMV-MITF expression constructs were provided by Christine Campbell (Cleveland Clinic Foundation, USA), Robert Benezra (Addgene plasmid #16061) and Yardena Samuels (Addgene plasmid #31151) respectively; the following constructs were previously described, pCMV Empty, pCMV-TBX3 DNA binding mutant, pCMV-TBX3 N-terminal, pCMV-TBX3 S720A and pCMV-TBX3 S720E expression constructs and *E-cadherin*-luciferase reporter construct (Peres et al., 2015, Willmer et al., 2016); pCMV-Flag-Empty, pCMV-Flag-Tbx3 and pCMV-Flag-Tbx3+2a (Willmer et al.,

1
2
3
4
5
6
7
8
9
10
11
12
13
14
15
16
17
18
19
20
21
22
23
24
25
26
27
28
29
30
31
32
33
34
35
36
37
38
39
40
41
42
43
44
45
46
47
48
49
50
51
52
53
54
55
56
57
58
59
60

2016) and pGL3-*IDI* and deletions of the *IDI* promoter (Singh et al., 2002). Mutations were introduced into the pGL3-*IDI* at -1986 bp by site-directed mutagenesis using the Stratagene QuickChange system.

Transfections and luciferase assays

Transfections were performed using Transfectin (Bio-Rad) and cell extracts assayed for firefly and *Renilla* luciferase activity using the dual luciferase assay system (Promega, Madison, WI) according to manufacturer’s instructions.

Small interfering RNA (siRNA)

Cells were transfected with si-*IDI*#1 (SASI_Hs01_00246328, Sigma, USA); si-*IDI*#2, (Dharmacon Lafayette, USA) or a non-silencing control siRNA (Qiagen, USA) using HiPerFect® (Qiagen, USA) according to manufacturer’s instructions.

Western blot analysis

Protein harvesting and western blotting was as described previously (Abrahams et al., 2008). Primary antibodies were: anti-TBX3 (AB99302, Abcam), anti-*IDI*1 (SC488, Santa Cruz Biotechnology, USA), anti-pAKT (9271, Cell Signalling Technology, USA), anti-AKT (9272, Cell Signalling Technology, USA), anti-p38 (MO800, Sigma, USA) and anti-HA (62-2, Sigma, USA) and anti-Flag (F1804, Sigma, USA).

DNA affinity immunoblot (DAI)

WT *IDI*1 (5'- CAGGTGCGCGCCACCACACCTGGCTAATTTTTC -3') and MT *IDI*1 (5'- CAGGTGCGCGCacCCA~~tgg~~CTGGCTAATTTTTC -3') oligonucleotides were annealed with their complementary strands. Biotinylated WT *IDI*1 oligonucleotide was immobilized on Dynabeads Streptavidin (Dyna Invitrogen) according to the manufacturer’s instructions and a DAI was performed as described (Willmer et al., 2016).

Electromobility shift assay (EMSA)

EMSA was performed as described (Li et al., 2013).

Chromatin immunoprecipitation (ChIP) assays

ChIP assays were carried out as described (Willmer et al., 2015).

Cell migration assay

Cell migration was measured using a two-dimensional scratch motility assay (Peres et al., 2010).

Transcriptomic analyses

TCGA melanoma cohort gene expression data (RNA-seq) was accessed via the cBioportal for Cancer Genomics (<http://www.cbioportal.org>) using CGDS-R (Gao et al., 2013). Individual gene expression values were retrieved as normalized RSEM (RNA-Seq by Expectation Maximization) and preprocessed using the TCGA/cBioportal projects. Upon log₂-transformation RSEM-values less than 1 were set to 1 if necessary. Melanoma samples were ordered by increasing expression values of averaged Verfaillie invasiveness signature (Verfaillie et al., 2015) or by *ID1* expression. The moving average expression of individual genes of interest, *TBX3* and *ID1*, was calculated with a sample window size of n=20 and trendlines added to the bar plots. The R-script for these analyses was described (Riesenberg et al., 2015). Co-expression gene correlation analyses between *MITF* and *E-cadherin* were performed. The significance of the Spearman rank correlation was determined using an asymptotic Spearman correlation test using original log₂ expression values and not the moving average values. RNA-seq data presented in Figure 6e were generated as described (Tsoi et al., 2018) and is available at the GEO using identifier GSE80829.

ChIP-seq data

ChIP-seq data for MITF binding to the *CDH1* locus was derived from the Gene Expression Omnibus dataset GSE77437 as previously described (Louphrasitthiphol et al., 2020) and visualised using the UCSC genome browser.

Statistical analysis

Statistical analyses were performed by parametric unpaired t-test (Excel, Microsoft, Redmond, WA, USA). Graphs plotted using GraphPad Prism software 6.0 (San Diego, CA). Data were obtained from three independent experiments. Error bars represent standard error of the mean (SEM) and significance was *p < 0.05, **p < 0.01, ***p < 0.001 and ****p < 0.0001.

DATA AVAILABILITY STATEMENT

Dataset related to this article can be found at <http://dx.doi.org/10.17632/w3y2445tw.1>, an open-source online data repository hosted at Mendeley Data (Peres et al., 2020).

ORCIDs

Jade Peres: <https://orcid.org/0000-0001-8568-4840>
Victoria Damerell: <https://orcid.org/0000-0003-0161-869X>
Jagat Chauhan: <https://orcid.org/0000-0003-4210-6260>
Ana Popovic: <https://orcid.org/0000-0003-3414-0573>
Pierre-Yves Desprez: <https://orcid.org/0000-0002-9880-4888>
Marie-Dominique Galibert: <https://orcid.org/0000-0003-0095-742X>
Colin R. Goding: <https://orcid.org/0000-0002-1614-3909>
Sharon Prince: <https://orcid.org/0000-0002-6975-5255>

CONFLICT OF INTEREST

The authors state no conflict of interest.

ACKNOWLEDGEMENTS

We would like to thank Prof Dorothy Bennett for the melanoma cell lines. The content is solely the responsibility of the authors and does not necessarily represent the official views of the funding agencies.

AUTHORS' CONTRIBUTIONS

Conceptualization: SP, JP, M-DG, CRG; Formal Analysis: SP, JP, VD, JC, CRG; Resources: SP, M-DG, PYD; Funding Acquisition: SP, M-GD, CRG; Investigation: SP, JP, VD, JC; Writing - Original Draft Preparation: SP, JP, M-DG, CRG, VD, AP.

FUNDING

This work was supported by grants from the South African Medical Research Council (SA MRC), the South African National Research Foundation (NRF), Cancer Association of South Africa (CANSA), the University of Cape Town (UCT), Centre National de la Recherche Scientifique (CNRS)/NRF and the Ludwig Institute for Cancer Research.

REFERENCES

- Abrahams A, Mowla S, Parker MI, Goding CR, Prince S. UV-mediated regulation of the anti-senescence factor Tbx2. *Journal of Biological Chemistry* 2008;283(4):2223-30.
- Boyd SC, Mijatov B, Pupo GM, Tran SL, Gowrishankar K, Shaw HM, et al. Oncogenic BRAFV600E signaling induces the T-box3 transcriptional repressor to repress E-cadherin and enhance melanoma cell invasion. *Journal of Investigative Dermatology* 2013;133(5):1269-77.
- Caramel J, Papadogeorgakis E, Hill L, Browne GJ, Richard G, Wierinckx A, et al. A switch in the expression of embryonic EMT-inducers drives the development of malignant melanoma. *Cancer cell* 2013;24(4):466-80.
- Carreira S, Goodall J, Denat L, Rodriguez M, Nuciforo P, Hoek KS, et al. Mitf regulation of D1a1 controls melanoma proliferation and invasiveness. *Cancer research* 2006;20(24):3426-39.
- Cheli Y, Giuliano S, Fenouille N, Allegra M, Hofman V, Hofman P, et al. Hypoxia and MITF control metastatic behaviour in mouse and human melanoma cells. *Oncogene* 2012;31(19):2461-70.
- Dantonio PM, Klein MO, FREIRE MR, Araujo CN, CHIACETTI AC, Correa RGJBR. Exploring major signaling cascades in melanomagenesis. 2019.
- Domingues B, Lopes JM, Soares P, Pópulo H. Melanoma treatment in review. *Immunotargets Ther* 2018;7:35.
- Eggermont AM, Spatz A, Robert C. Cutaneous melanoma. *The Lancet* 2014;383(9919):816-27.
- Falletta P, Sanchez-del-Campo L, Chauhan J, Efferen M, Kenyon A, Kershaw CJ, et al. Translation reprogramming is an evolutionarily conserved driver of phenotypic plasticity and therapeutic resistance in melanoma. *Genes development* 2017;31(1):18-33.
- Feige E, Yokoyama S, Levy C, Khaled M, Igras V, Lin RJ, et al. Hypoxia-induced transcriptional repression of the melanoma-associated oncogene MITF. *Proceedings of the National Academy of Sciences* 2011;108(43):E924-E33.
- Gao J, Aksoy BA, Dogrusoz U, Dresdner G, Gross B, Sumer SO, et al. Integrative analysis of complex cancer genomics and clinical profiles using the cBioPortal. *Sci Signal* 2013;6(269):pl1-pl.
- Gil J, Betancourt LH, Pla I, Sanchez A, Appelqvist R, Miliotis T, et al. Clinical protein science in translational medicine targeting malignant melanoma. *Cell Biology and Toxicology* 2019;35(4):293-332.
- Goding CR, Arnheiter H. MITF—the first 25 years. *Genes & Development* 2019;33(15-16):983-1007.
- Hoek KS, Schlegel NC, Brafford P, Sucker A, Ugurel S, Kumar R, et al. Metastatic potential of melanomas defined by specific gene expression profiles with no BRAF signature. *Pigment Cell Research* 2006;19(4):290-302.
- Khan SF, Damerell V, Omar R, Du Toit M, Khan M, Maranyane H, et al. The roles and regulation of TBX3 in development and disease. *Gene* 2019:144223.
- Kozar I, Margue C, Rothengatter S, Haan C, Kreis S. Many ways to resistance: How melanoma cells evade targeted therapies. *Biochimica et Biophysica Acta (BBA) - Reviews on Cancer* 2019.
- Landsberg J, Kohlmeyer J, Renn M, Bald T, Rogava M, Cron M, et al. Melanomas resist T-cell therapy through inflammation-induced reversible dedifferentiation. *Nature* 2012;490(7420):412-6.
- Lee J, Kim K, Kim JH, Jin HM, Choi HK, Lee S-H, et al. Id helix-loop-helix proteins negatively regulate TRANCE-mediated osteoclast differentiation. *Blood* 2006;107(7):2686-93.

- Li J, Weinberg MS, Zerbini L, Prince S. The oncogenic TBX3 is a downstream target and mediator of the TGF- β 1 signaling pathway. *J Molecular biology of the cell* 2013;24(22):3569-76.
- Lideikaitė A, Mozūraitienė J, Letautienė S. Analysis of prognostic factors for melanoma patients. *Acta Med Litu* 2017;24(1):25.
- Louphrasitthiphol P, Ledaki I, Chauhan J, Falletta P, Siddaway R, Buffa FM, et al. MITF controls the TCA cycle to modulate the melanoma hypoxia response. *Pigment cell melanoma research* 2019;32(6):792-808.
- Louphrasitthiphol P, Siddaway R, Loffreda A, Pogenberg V, Friedrichsen H, Schepsky A, et al. Tuning transcription factor availability through acetylation-mediated genomic redistribution. *Molecular cell* 2020;In press.
- Mansky KC, Marfatia K, Purdom GH, Luchin A, Hume DA, Ostrowski MC. The microphthalmia transcription factor (MITF) contains two N-terminal domains required for transactivation of osteoclast target promoters and rescue of mi mutant osteoclasts. *Journal of leukocyte biology* 2002;71(2):295-303.
- Miller AJ, Mihm MC. Melanoma. *New England Journal of Medicine* 2006;355(1):51-65.
- O'Donnell JS, Long GV, Scolyer RA, Teng MW, Smyth MJ. Resistance to PD1/PDL1 checkpoint inhibition. *J Cancer treatment reviews* 2017;52:71-81.
- Peres J, Davis E, Mowla S, Bennett DC, Li JA, Wansleben S, et al. The highly homologous T-Box transcription factors, TBX2 and TBX3, have distinct roles in the oncogenic process. *Genes and Cancer* 2010;1(3):272-82.
- Peres J, Galibert M-D, Prince S. TBX3 whole genome microarray dataset. *Mendeley Data* 2020;1.
- Peres J, Mowla S, Prince S. The T-box transcription factor, TBX3, is a key substrate of AKT3 in melanomagenesis. *Oncotarget* 2015;6(3):1821.
- Peres J, Prince S. The T-box transcription factor, TBX3, is sufficient to promote melanoma formation and invasion. *Molecular Cancer* 2013;12(1):117.
- Poser I, Bosserhoff AK. Transcription factors involved in development and progression of malignant melanoma. *Histology histopathology* 2004.
- Rambow F, Marine J-C, Goding CR. Melanoma plasticity and phenotypic diversity: therapeutic barriers and opportunities. *Genes & Development* 2019;33(19-20):1295-318.
- Riesenberg S, Groetchen A, Siddaway R, Bald T, Reinhardt J, Smorra D, et al. MITF and c-Jun antagonism interconnects melanoma dedifferentiation with pro-inflammatory cytokine responsiveness and myeloid cell recruitment. *Nature communications* 2015;6:8755.
- Rodriguez M, Aladowicz E, Lanfranccone L, Goding CR. Tbx3 represses E-cadherin expression and enhances melanoma invasiveness. *Cancer research* 2008;68(19):7872-81.
- Roschger C, Cabrele C. The Id-protein family in developmental and cancer-associated pathways. *Cell Communication Signaling* 2017;15(1):7.
- Scolyer RA, Prieto VG, Elder DE, Cochran AJ, Mihm MC. Classification and Histopathology of Melanoma. *Cutaneous Melanoma* 2020:317-79.
- Singh J, Murata K, Itahana Y, Desprez P-Y. Constitutive expression of the Id-1 promoter in human metastatic breast cancer cells is linked with the loss of NF-1/Rb/HDAC-1 transcription repressor complex. *Oncogene* 2002;21(12):1812-22.
- Straume O, Akslen L. Strong expression of ID1 protein is associated with decreased survival, increased expression of ephrin-A1/EPHA2, and reduced thrombospondin-1 in malignant melanoma. *British journal of cancer* 2005;93(8):933-8.
- Sviderskaya EV, Kallenberg DM, Bennett DC. The wellcome trust functional genomics cell bank: Holdings. *J Pigment cell melanoma research* 2010;23(1):147-50.

- 1
2
3 Tsoi J, Robert L, Paraiso K, Galvan C, Sheu KM, Lay J, et al. Multi-stage differentiation
4 defines melanoma subtypes with differential vulnerability to drug-induced iron-
5 dependent oxidative stress. *Cancer cell* 2018;33(5):890-904. e5.
6
7 Verfaillie A, Imrichova H, Atak ZK, Dewaele M, Rambow F, Hulselmans G, et al. Decoding
8 the regulatory landscape of melanoma reveals TEADS as regulators of the invasive cell
9 state. *Nature communications* 2015;6:6683.
10
11 Willmer T, Hare S, Peres J, Prince S. The T-box transcription factor TBX3 drives proliferation
12 by direct repression of the p21 WAF1 cyclin-dependent kinase inhibitor. *Cell division*
13 2016;11(1):6.
14
15 Willmer T, Peres J, Mowla S, Abrahams A, Prince S. The T-Box factor TBX3 is important in
16 S-phase and is regulated by c-Myc and cyclin A-CDK2. *Cell Cycle* 2015;14(19):3173-
17 83.
18
19 Zigler M, Villares GJ, Dobroff AS, Wang H, Huang L, Braeuer RR, et al. Expression of Id-1
20 is regulated by MCAM/MUC18: a missing link in melanoma progression. *Cancer*
21 *research* 2011;71(10):3494-504.
22
23
24
25
26
27
28
29
30
31
32
33
34
35
36
37
38
39
40
41
42
43
44
45
46
47
48
49
50
51
52
53
54
55
56
57
58
59
60

FIGURE LEGENDS

Figure 1 Genes differentially expressed in ME1402 VGP melanoma shCtrl and shTBX3 cells.

(a, d) qRT-PCR was performed using primers specific to the indicated genes and levels were normalised to GUSB. (b, e) Western blot analyses using antibodies specific to TBX3 and p38 (loading control). Densitometric readings were obtained and protein expression levels are represented as a ratio of protein of interest/p38. (c) Two-dimensional hierarchical cluster heat map and volcano plot showing differential gene expression. Levels of expression are indicated on a colour scale (Z score scale); yellow (upregulated) and red (downregulated) genes. Gene lists 1 and 2 of the differentially expressed genes are shown in Supplementary Table S1. Table lists the genes selected for validation by qRT-PCR in (d-e) and shown as log fold expression. (a,d-e) Data are the mean±SEM of three independent experiments (*p<0.05; **p<0.01).

Figure 2 Positive correlation between TBX3 and ID1 levels and to the Verfaillie invasive melanoma signature.

(a-b) Protein extracts from indicated cell lines were subjected to western blot analyses with antibodies specific to TBX3, ID1 and p38 (loading control). Densitometry readings were obtained using UN-SCAN-IT graph digitizer and protein expression levels are represented as a ratio of protein of interest/p38. (c-d) The Cancer Genome Atlas (TCGA) melanoma samples (black line) were scored and ranked according to the Verfaillie invasive gene signature (Verfaillie et al., 2015). Vertical grey lines indicate expression of the indicated gene in each melanoma sample. The purple line indicates the moving average of (c) *TBX3* or (d) *ID1* mRNA expression across 20 melanomas.

Figure 3 TBX3 is a direct transcriptional activator of ID1 in VGP melanoma cells.

(a-e) Luciferase assays of cells co-transfected with the *E-cadherin*- or *ID1*- luciferase reporter constructs and, unless otherwise stated, 100 ng TBX3 expression constructs. Luciferase activity was measured and *ID1* fold activation calculated. (f) EMSAs using ME1402 nuclear extract and biotinylated *ID1* oligonucleotides. Competition reactions were performed with unlabelled random oligonucleotides. Supershifted complexes were incubated with a TBX3 antibody. Specific complexes, arrow, and unspecific complexes, NS. (g) ChIP assays of ME1402 DNA immunoprecipitated with TBX3 or IgG (negative control) antibodies and assayed by qRT-PCR; *GAPDH* (negative control). (a-e, g) Data are the mean±SEM of three independent experiments (*p<0.05; **p<0.01; ***p<0.001).

Figure 4 AKT pathway enhances the ability of TBX3 to bind and activate *ID1* in VGP melanoma cells.

(a) Luciferase assays of cells co-transfected with the *ID1* promoter luciferase reporter and the indicated constructs. Luciferase activity was measured and *ID1* fold activation calculated. Data are the mean±SEM of three independent experiments (* $p < 0.05$; *** $p < 0.001$). (a, lower panel) Western blot analysis showing expression of the various constructs transfected. (b-c) DAI assays were performed using lysates from ME1402 melanoma cells (b) treated with an AKT inhibitor and incubated with biotinylated WT or MT *ID1* oligonucleotides or (c) transfected with Empty, WT TBX3, TBX3 S720A or TBX3 S720E and incubated with biotinylated WT *ID1* oligonucleotides. Pull-down assays were performed using streptavidin magnetic beads and lysates were subjected to western blotting. (b-c, lower panels) Western blot analyses. Densitometric readings values were determined as described in Figure 1.

Figure 5 TBX3 promotes cell migration through the activation of *ID1*.

(a-c) Scratch motility assays were performed for (a) VGP melanoma cells transfected with si-*ID1* #1, si-*ID1* #2 or si-Ctrl for 48 hrs; (b) VGP melanoma cells transfected with si-TBX3/si-Ctrl and/or with an *ID1* expression construct (referred to as *ID1*) for 48 hrs and (c) WM1650-Ctrl and -TBX3 overexpressing RGP melanoma cells transfected with si-*ID1* #1, si-*ID1* #2 or si-Ctrl for 48 hrs. Histograms in (a) and (c) show the distance migrated and in (b) the fold change migrated. Data are the mean±SEM of three independent experiments (* $p < 0.05$, ** $p < 0.01$, *** $p < 0.001$, **** $p < 0.0001$). Microscopic images show the scratches at 0 and 24 hrs. Western blot analyses. Densitometric readings values were determined as described in Figure 1.

Figure 6 *ID1* prevents activation of *E-cadherin* by *MITF*.

(a) Luciferase, (b) qRT-PCR; and (c) Co-immunoprecipitation assays. (d) TCGA melanoma samples (black line) scored and ranked according to *ID1*. Vertical grey lines; *MITF* levels in each sample. Blue line; moving *MITF* average. (e) Heatmap: relative genes expression from RNA-seq (GSE80829) of 53 melanoma cell lines grouped according to phenotype. (f) UCSC genome browser screenshot showing *MITF* ChIP-seq (GSE77437). (g) ChIP assays of ME1402 cells co-transfected with FLAG-Empty or FLAG-*MITF* constructs and either siCtrl or si-*ID1*. DNA immunoprecipitated with FLAG or IgG (negative control) was assayed by qRT-PCR with primers spanning sites 1 and 2 in *CDH1*. qRT-PCR (h) Scratch motility assays. (i)

1
2
3
4
5
6
7
8
9
10
11
12
13
14
15
16
17
18
19
20
21
22
23
24
25
26
27
28
29
30
31
32
33
34
35
36
37
38
39
40
41
42
43
44
45
46
47
48
49
50
51
52
53
54
55
56
57
58
59
60

Correlation analyses. (a, b, h, g) Data are the mean±SEM (*p < 0.05, **p < 0.01, ***p < 0.001, ****p < 0.0001).

SUPPLEMENTARY MATERIAL

Supplementary Table S1. List of genes differentially expressed (2-fold variance threshold) and are shown in two sets, Gene list 1 and Gene list 2 as shown in the Heat map in Figure 1c.

Supplementary Table S2. Genes upregulated in ME1402 shTBX3 cells compared to shCtrl cells with reported functions in migration and invasion. Lowest false discovery rate (FDR) was used in all analyses (≤ 0.2) and a fold change (FC) of ≥ 2 .

Supplementary Table S3. Genes downregulated in ME1402 shTBX3 cells compared to shCtrl cells with reported functions in migration and invasion. Lowest FDR was used in all analyses (≤ 0.2) and a FC of ≥ 2 .

Supplementary Table S4. The known genetic mutation status of the melanoma cell lines used in this study.

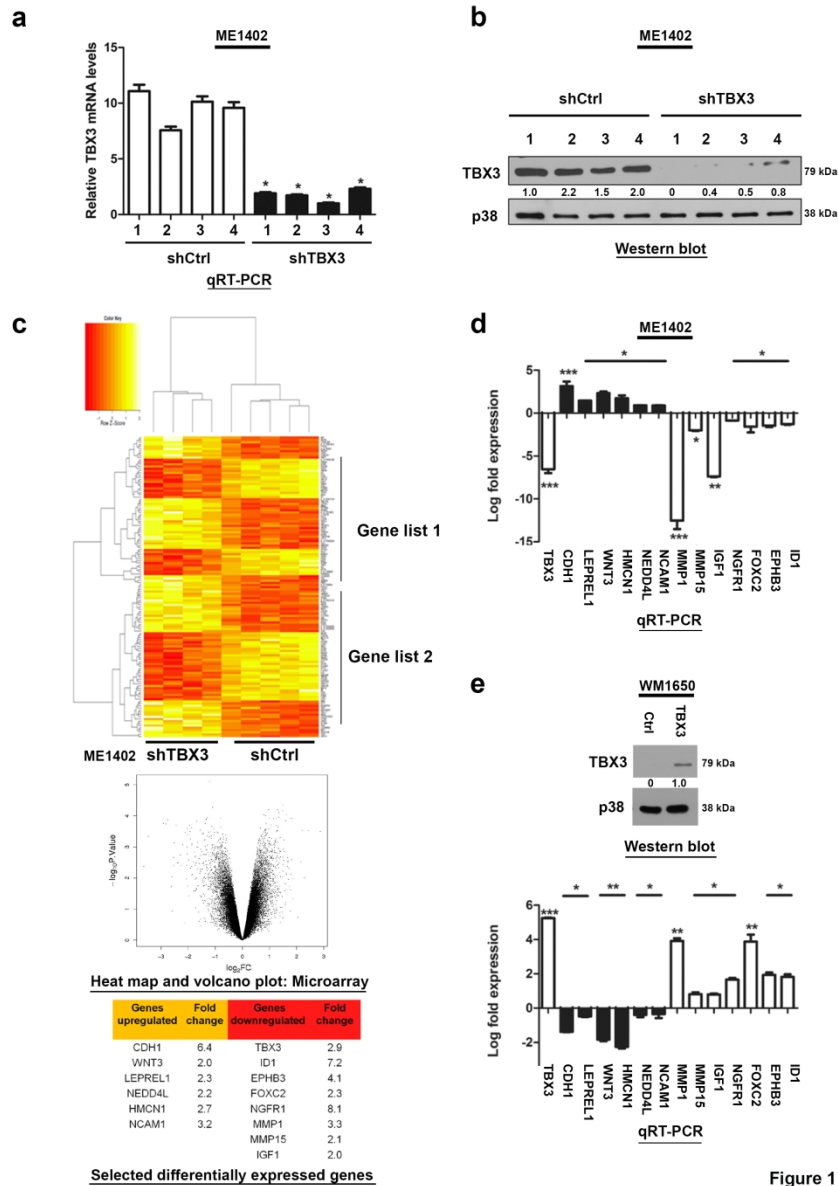


Figure 1

Figure 1 Genes differentially expressed in ME1402 VGP melanoma shCtrl and shTBX3 cells. (a, d) qRT-PCR was performed using primers specific to the indicated genes and levels were normalised to GUSB. (b, e) Western blot analyses using antibodies specific to TBX3 and p38 (loading control). Densitometric readings were obtained and protein expression levels are represented as a ratio of protein of interest/p38. (c) Two-dimensional hierarchical cluster heat map and volcano plot showing differential gene expression. Levels of expression are indicated on a colour scale (Z score scale); yellow (upregulated) and red (downregulated) genes. Gene lists 1 and 2 of the differentially expressed genes are shown in Supplementary Table S1. Table lists the genes selected for validation by qRT-PCR in (d-e) and shown as log fold expression. (a,d-e) Data are the mean±SEM of three independent experiments (*p<0.05; **p<0.01).

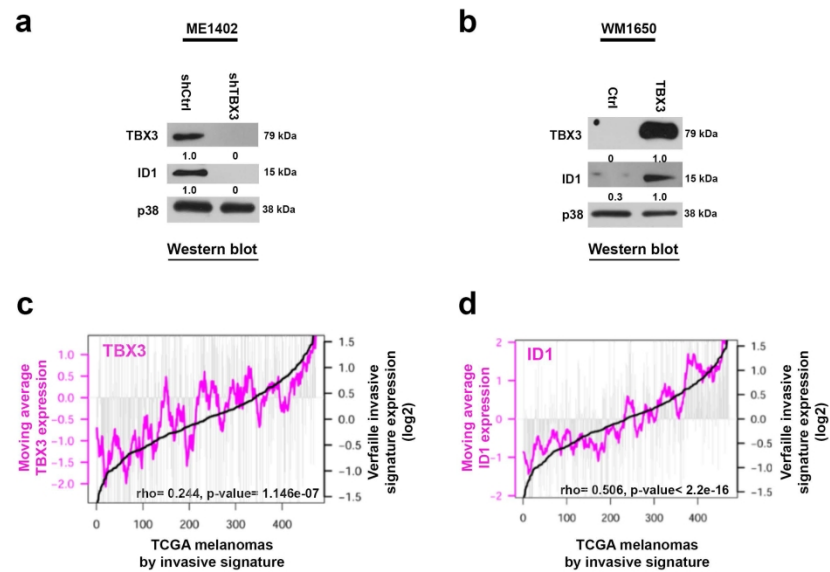


Figure 2

Figure 2 Positive correlation between TBX3 and ID1 levels and to the Verfaillie invasive melanoma signature. (a-b) Protein extracts from indicated cell lines were subjected to western blot analyses with antibodies specific to TBX3, ID1 and p38 (loading control). Densitometry readings were obtained using UN-SCAN-IT graph digitizer and protein expression levels are represented as a ratio of protein of interest/p38. (c-d) The Cancer Genome Atlas (TCGA) melanoma samples (black line) were scored and ranked according to the Verfaillie invasive gene signature (Verfaillie et al., 2015). Vertical grey lines indicate expression of the indicated gene in each melanoma sample. The purple line indicates the moving average of (c) TBX3 or (d) ID1 mRNA expression across 20 melanomas.

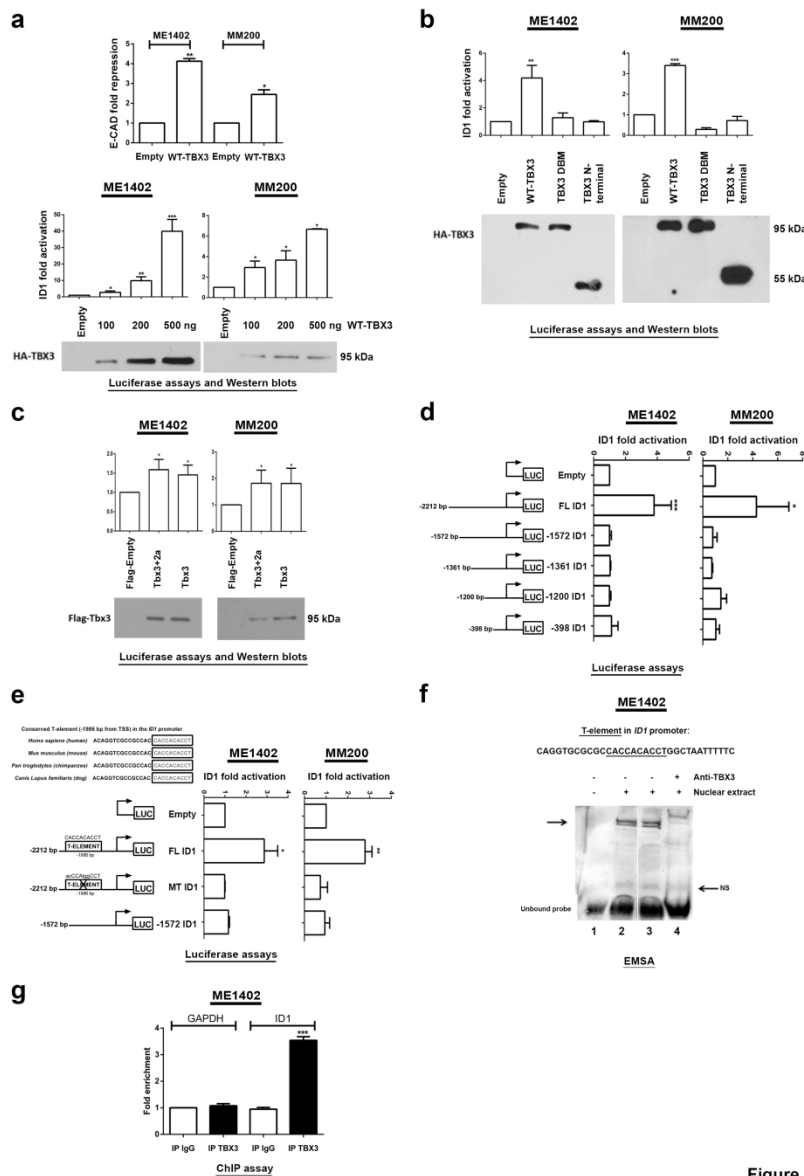


Figure 3

Figure 3 TBX3 is a direct transcriptional activator of ID1 in VGP melanoma cells. (a-e) Luciferase assays of cells co-transfected with the E-cadherin- or ID1- luciferase reporter constructs and, unless otherwise stated, 100 ng TBX3 expression constructs. Luciferase activity was measured and ID1 fold activation calculated. (f) EMSAs using ME1402 nuclear extract and biotinylated ID1 oligonucleotides. Supershifted complexes were incubated with a TBX3 antibody. Specific complexes, arrow, and unspecific complexes, NS. (g) ChIP assays of ME1402 DNA immunoprecipitated with TBX3 or IgG (negative control) antibodies and assayed by qRT-PCR; GAPDH (negative control). (a-e, g) Data are the mean \pm SEM of three independent experiments (* p <0.05; ** p <0.01; *** p <0.001).

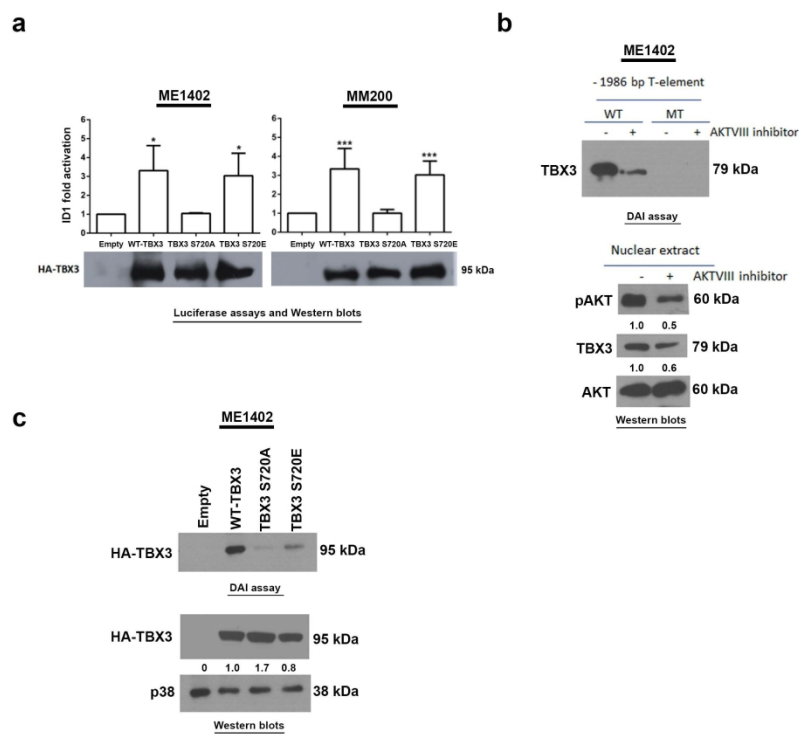


Figure 4

Figure 4 AKT pathway enhances the ability of TBX3 to bind and activate ID1 in VGP melanoma cells. (a) Luciferase assays of cells co-transfected with the ID1 promoter luciferase reporter and the indicated constructs. Luciferase activity was measured and ID1 fold activation calculated. Data are the mean±SEM of three independent experiments (*p<0.05; ***p<0.001). (a, lower panel) Western blot analysis showing expression of the various constructs transfected. (b-c) DAI assays were performed using lysates from ME1402 melanoma cells (b) treated with an AKT inhibitor and incubated with biotinylated WT or MT ID1 oligonucleotides or (c) transfected with Empty, WT TBX3, TBX3 S720A or TBX3 S720E and incubated with biotinylated WT ID1 oligonucleotides. Pull-down assays were performed using streptavidin magnetic beads and lysates were subjected to western blotting. (b-c, lower panels) Western blot analyses. Densitometric readings values were determined as described in Figure 1.

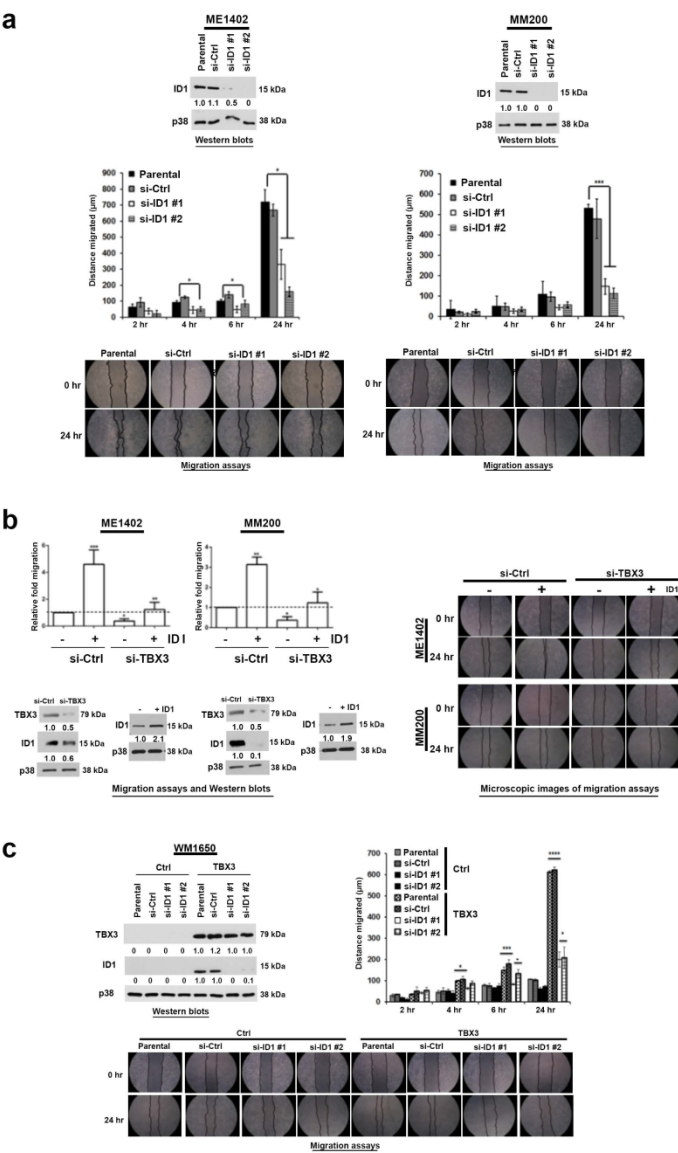


Figure 5

Figure 5 TBX3 promotes cell migration through the activation of ID1. (a-c) Scratch motility assays were performed for (a) VGP melanoma cells transfected with si-ID1 #1, si-ID1 #2 or si-Ctrl for 48 hrs; (b) VGP melanoma cells transfected with si-TBX3/si-Ctrl and/or with an ID1 expression construct (referred to as ID1) for 48 hrs and (c) WM1650-Ctrl and -TBX3 overexpressing RGP melanoma cells transfected with si-ID1 #1, si-ID1 #2 or si-Ctrl for 48 hrs. Histograms in (a) and (c) show the distance migrated and in (b) the fold change migrated. Data are the mean±SEM of three independent experiments (*p < 0.05, **p < 0.01, ***p < 0.001, ****p < 0.0001). Microscopic images show the scratches at 0 and 24 hrs. Western blot analyses. Densitometric readings values were determined as described in Figure 1.

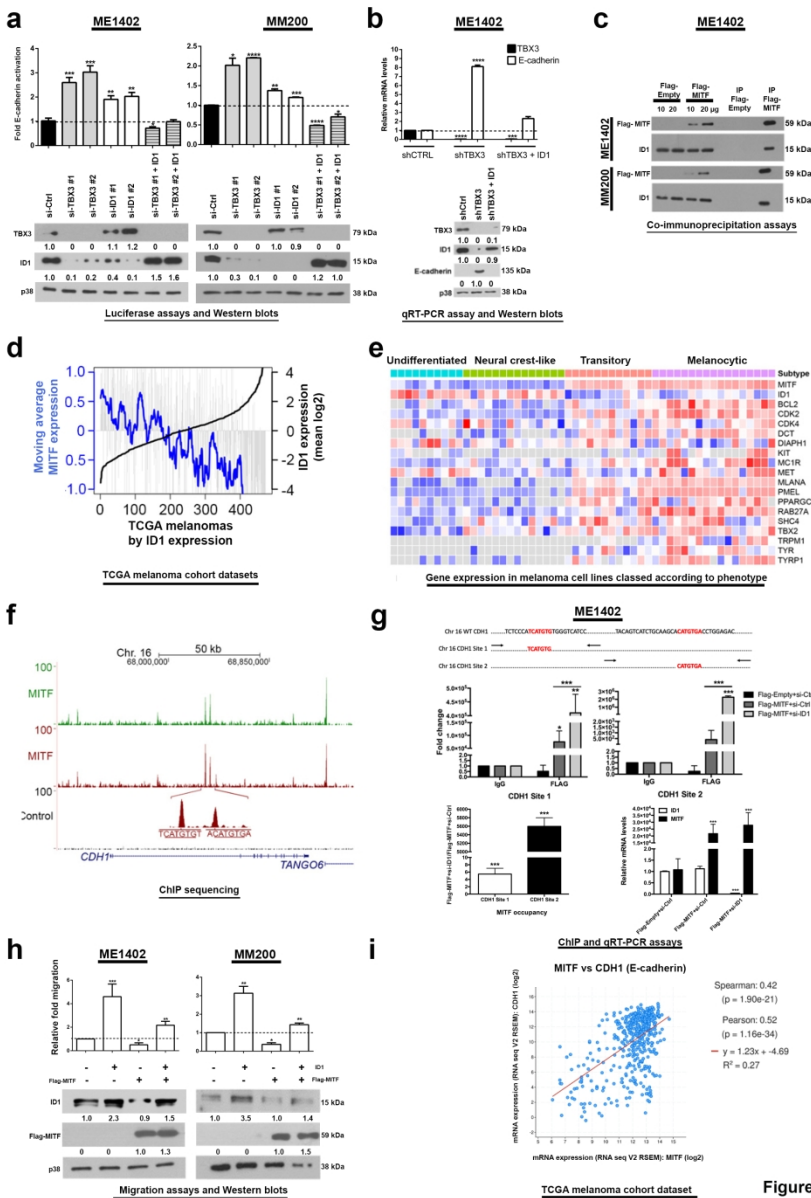


Figure 6

Figure 6 ID1 prevents activation of E-cadherin by MITF. (a) Luciferase, (b) qRT-PCR; and (c) Co-immunoprecipitation assays. (d) TCGA melanoma samples (black line) scored and ranked according to ID1. Vertical grey lines; MITF levels in each sample. Blue line; moving MITF average. (e) Heatmap: relative genes expression from RNA-seq (GSE80829) of 53 melanoma cell lines grouped according to phenotype. (f) UCSC genome browser screenshot showing MITF ChIP-seq (GSE77437). (g) ChIP assays of ME1402 cells co-transfected with FLAG-Empty or FLAG-MITF constructs and either siCtrl or si-ID1. DNA immunoprecipitated with FLAG or IgG (negative control) was assayed by qRT-PCR with primers spanning sites 1 and 2 in CDH1. qRT-PCR (h) Scratch motility assays. (i) Correlation analyses. (a, b, h, g) Data are the mean±SEM (*p < 0.05, **p < 0.01, ***p < 0.001, ****p < 0.0001).

Gene list 1	Gene list 2
MET	KCNJ13
ABCB4	ETNK1
LOC441288	LAMB2P1
PTPRZ1	LOC202781
NEDD4L	8CN4B
CER81	AC8L8
CCNB1IP1	PAQR6
FABP7	LRRN4CL
DNAJB1	WIPF3
8H2B3	LRRC24
PEKFB4	C1QTNF4
PEA16	DAK
PMEP1A	IGDCC4
ID3	DDX26
PLEC	CDH1
FGFR1	ABC89
RNF187	CCDC84
ENO2	METTL7B
RBM19	TBX3
FO8L1	H81BP3
PLXNB3	ULBP2
MAP2K3	OA83
TRPV4	EPHB3
BAG3	MMP1
ID1	KRT8B
IGF1	PAFAH2
FAM176A	ZNF880
LEPREL1	RA88F7
MMAB	CCDC88
8LC35B4	ECE1
BEGAIN	8P140L
8GCD	ZC3HAV1
FBR8L1	8YTL4
CNP	GLI2
CACNA1H	KIAA1949
HMCN1	ZNF628
T8PAN14	CCDC81
NCAM1	8ERPIND1
TRAPPC8A	H8BP1L1
CPT1C	KIAA1244
THY1	MAP1A
8MARCA1	MB
ZAF837	CD34
DPY8L2	FOXO2
8DC3	FHDC1
ADAM19	LYPD1
88BP3	AMN1
RHOB	8YT7
NGFR1	ARHGAP24
MMP15	RBP7
KCNN4	ANKRD28P1
TIMP3	FBXL17
ND1	ABCA1
ACTN1	LOC100130016
8H3BGR13	HTR2B
LOC845591	CAND2
WNT3	8LC2A4
CB8	8ELV
8EMA6A	LOC284960
8NAI2	MIG7
TDO2	PPP1R14A
OR61V1	

Supplementary Table S1. List of genes differentially expressed (2-fold variance threshold) and are shown in two sets, Gene list 1 and Gene list 2 as shown in the Heat map in Figure 1c.

104x147mm (300 x 300 DPI)

	Gene Symbol	Gene Name	FC ≥2	FDR	Description	References for description of genes
1	CDH1	E-cadherin	6.37	0.09	Promotes cell adhesion	Rodriguez et. al., 2008
2	WNT3	Wingless-type MMTV integration site family, member 3	2.00	0.09	Tumour suppressor and inhibits WNT signalling pathway	Polakis, 2000
3	LEPREL1	Leprecan-like 1	2.28	0.09	Tumour suppressor	Shah et. al., 2009
4	NEDD4L	Neural precursor cell expressed, developmentally down-regulated 4-like	2.17	0.09	Tumour suppressor	Kovacevic et. al., 2012
5	HMCN1	Hemicentin 1	2.66	0.09	Tumour suppressor	Argraves et. al., 2003
6	NCAM1	Neural cell adhesion molecule 1	3.14	0.09	Tumour suppressor gene in Melanoma	Roesler et al., 1997

Supplementary Table S2. Genes upregulated in ME1402 shTBX3 cells compared to shCtrl cells with reported functions in migration and invasion. Lowest false discovery rate (FDR) was used in all analyses (≤0.2) and a fold change (FC) of ≥2.

104x147mm (300 x 300 DPI)

	Gene Symbol	Gene Name	FC ≥2	FDR	Description	References for description of genes
1	ID1	Inhibitor of DNA binding 1, dominant negative helix-loop-helix protein	7.21	0.09	Promotes tumour cell migration and invasion	Alani et.al., 2010, Zigler et.al., 2011
2	EPHB3	EPH receptor B3	4.11	0.09	Promotes tumour metastasis by enhancing cell survival and migration	Ji et.al., 2011
3	FOXC2	Forkhead box C2 (MFH-1, mesenchyme forkhead 1	2.33	0.09	Promotes tumour formation and angiogenesis	Mani et.al., 2007, Kume, 2012
4	NGFR	Nerve growth factor receptor	8.06	0.09	Induces invasion and metastasis in glioma and melanoma	Marchetti et al., 2004; Johnston et al., 2007
5	MMP1	Metalloprotease 1	3.34	0.12	Promotes cell migration	Kim et al., 2011
6	MMP15	Metalloprotease 15	2.11	0.2	Promotes cell migration	Tao et al., 2011
7	IGF1	Insulin like growth factor 1	2.00	0.1	Promotes cell migration and invasion	Capoluongo, 2011.

Supplementary Table S3. Genes downregulated in ME1402 shTBX3 cells compared to shCtrl cells with reported functions in migration and invasion. Lowest FDR was used in all analyses (≤0.2) and a FC of ≥2.

Cell line	Mutation status	References
ME1402 (VGP)	BRAF V600E	Pavey et al. 2004
MM200 (VGP)	BRAF V600E PTEN F56I	Stark & Hayward et al. 2007 Pavey et al. 2004
WM1650 (RGP)	-	Herlyn et al. 1989 Part of: Wistar Institute melanoma cell line collection.

Supplementary Table S4. The known genetic mutation status of the melanoma cell lines used in this study.

209x295mm (300 x 300 DPI)